Journal of Catalysis 267 (2009) 40–49

Contents lists available at ScienceDirect

Journal of Catalysis

journal homepage: www.elsevier.com/locate/jcat

Influence of K-doping on a $Pd/SiO_2–Al_2O_3$ catalyst

R. Pellegrini [a], G. Leofanti [a,b], G. Agostini [c,d], L. Bertinetti [c,d], S. Bertarione [c,d], E. Groppo [c,d,*], A. Zecchina [c,d], C. Lamberti [c,d]

[a] Chimet SpA – Catalyst Division, Via di Pescaiola 74, Viciomaggio Arezzo I-52041, Italy
[b] Consultant, Via Firenze 43, 20010 Canegrate, Milano, Italy
[c] Dipartimento di Chimica IFM, Università di Torino, Via P. Giuria 7, I-10125 Torino, Italy
[d] NIS Centre of Excellence, Università di Torino, Via P. Giuria 7, I-10125 Torino, Italy

ARTICLE INFO

Article history:
Received 20 March 2009
Revised 1 June 2009
Accepted 19 July 2009
Available online 22 August 2009

Keywords:
Pd-supported catalyst
Hydrogenation reactions
Particle size distribution
Metal support interaction
TEM
CO chemisorption
Poisoning

ABSTRACT

This work is devoted to understand the effect of K-doping (from K_2CO_3) on the reducibility, sintering, and surface properties of Pd metal nanoparticles deposited on a peculiar high surface area $SiO_2–Al_2O_3$ (SA) support. The effect of K-doping on the Pd/SA catalyst is systematically investigated by means of several complementary techniques (TPR, TEM, CO chemisorption and FTIR spectroscopy), trying to separate the effects of the doping loading (spanning the large 0.25–20.3 K/Pd atomic ratio interval), of the activation temperature (up to 823 K) and of the activation atmosphere (air or H_2). It is shown that the presence of dopant, already at the lowest loading, causes an important increase of the PdO reduction temperature. The sulphur poisoning released from the support in the undoped sample during the thermal treatments in H_2 atmosphere is inhibited in the presence of K_2CO_3. The dramatic loss of metal area measured by CO chemisorption for samples H_2-treated at high temperature is not justified by the small particle sintering observed by TEM, and is assigned to the progressive particle encapsulation due to the mobilization of the support by reaction between carbonate and support itself. FTIR spectroscopy of adsorbed CO, allowing to probe the nature of the Pd surface available for adsorption, confirms the hypothesis.

© 2009 Elsevier Inc. All rights reserved.

1. Introduction

Palladium exhibits good catalytic properties in hydrogenation reactions that make it widely used in fine chemical synthesis [1,2]. In this context, the product selectivity is the key factor in determining the quality of a catalyst. In general, to induce selectivity other components must be added to the pristine metal catalyst, resulting in a complex nanomaterial with properties not present in the precursor [3]. A possible strategy can be a preliminary modification of the proportion of surface hydrogen species by employing bimetallic alloys (e.g. Pd–Au or Pt–Au) instead of the pure metal. The use of bimetallic catalysts can also be a way to increase the resistance to the particle sintering, and to change the geometry and the electronic properties of the active sites [4–6]. A second common practice to attain selectivity is to design a specific reaction path for the reactant/product molecules by addition of proper additives called promoters, modifiers, or dopants [7–10]. For example, Zn addition on Pd/Al_2O_3 catalyst modifies the turnover rate of the water–gas shift reaction [11], while the hydrogenation of phenol to cyclohexanone [12–15], the selective hydrogenation of acetylene to ethylene [16,17] and the conversion of syn-gas to methanol [18–20] require alkali- and alkaline earth-doped palladium catalysts. In this regard, it has been shown that modifying additives such as Ce, Zr, La and Cs oxides have influence on the electronic state of palladium supported on γ-Al_2O_3 [21].

Notwithstanding the fact that alkali metal promoters are successfully used since several decades [22], their effective overall role is still debated [13,23,24]. Together with a pure geometrical effect on the accessibility of the metal particles surface, in fact, alkali metal promoters can also influence the electronic structure of the metal particles and their mobility on the support, thus facilitating or preventing their sintering during the thermal treatments. Moreover, the contact between the doping species and the support may cause modifications to the support itself that can affect the availability of the metal particles for the catalytic process to take place. In fact, the metal particles may be covered by dissolved support material, or by the shrinkage of the porous system of the support. Furthermore, the metal particles may undergo doping by foreign species other than the added doping salt, but coming from the support [25]. It is thus clear that a complete understanding of the effect of promoters in modifying the catalyst's properties implies the investigation of all these different phenomena.

Very recently, we have investigated the morphological modifications undergone by a silicoaluminate support (SA) during all

* Corresponding author. Fax: +39 011 6707855.
E-mail address: elena.groppo@unito.it (E. Groppo).

0021-9517/$ - see front matter © 2009 Elsevier Inc. All rights reserved.
doi:10.1016/j.jcat.2009.07.008

the steps of catalyst preparation (i.e. Pd deposition, thermal treatments and doping by K_2CO_3) [26]. In particular, it has been demonstrated that the support is highly mobilized by the addition of K_2CO_3 dopant, and that the modifications of the support increase upon increasing the dopant concentration and the activation temperature. It is expected that the processes affecting the SA support have influence also on the Pd particles, in terms of (i) Pd particle formation, (ii) Pd particle size, and (iii) fraction and properties of the available Pd surface atoms. In the present work, the effect of K-doping on the catalyst is systematically investigated by means of several complementary techniques (TPR, TEM, CO chemisorption and FTIR spectroscopy), trying to separate the effects of the activation temperature and atmosphere (H_2 and air) and of K concentration.

The system investigated here represents an example where the particle size distribution measured by TEM, often referred to as dispersion, does not match with the surface sites really available as measured by CO chemisorption. This apparent disagreement is due to the co-presence of several different effects, involving not only the Pd particles but also the support itself (such as particle sintering, lost of surface sites due to particle encapsulation, or poisoning). Most of the metal-supported real catalysts present a similar high degree of complexity which must be understood in order to determine the structure–reactivity relationship. To achieve this goal more than one technique has to be adopted, such as TEM, chemisorption and FTIR of adsorbed species. Each specific technique has its own advantages and limits; consequently, the critical use of several independent techniques is strongly recommended in order to get a complete catalyst characterization [27].

2. Experimental

2.1. Sample preparation and nomenclature

A sodium-neutralized silica–alumina (SA in the following) with a SiO_2/Al_2O_3 ratio of 5.7 was used as support. Undoped Pd catalysts (Pd_{und} in the following) was prepared by the deposition-precipitation method [28,29]. Briefly, palladium hydroxide was deposited onto the support using Na_2PdCl_4 as a palladium precursor and Na_2CO_3 as basic agent. The supported palladium hydroxide was then water-washed until residual chlorides were removed and dried at 393 K overnight. Final Pd_{und} catalyst contained 2.05% Pd and some impurities arising from SA (Na 2.64%, K 0.04%, Ca 0.05%, Mg 0.04% and S < 0.10%). It had a surface area of 141 m^2/g and a pore volume of 0.83 cm^3/g, as evaluated by N_2 adsorption measurements [26,30].

K-doped catalysts were prepared by dry impregnation of corresponding undoped catalysts with aqueous solution of dopant compounds (namely carbonate, hydroxide and chloride), followed by drying in a static oven for 16 h at 393 K. Supported metal particles were then obtained via the thermal reduction of the precursor in H_2 atmosphere, in either dynamic or static conditions, depending on the characterization technique. In order to follow the clustering of the metal particles three reduction temperatures were investigated: 393 K, 673 K and 823 K. Moreover, some doped catalysts were submitted to washing with water in order to remove the soluble fraction. Washing was done using water at 45 °C inside a sintered disc filter funnel. The investigated samples had K/Pd atomic ratios of 0, 0.25, 0.60, 1.0, 4.3, 10.0 and 20.3, hereafter labelled as Pd_{und}, PdK0.2, PdK0.6, PdK1, PdK4, PdK10 and PdK20, respectively. The adopted nomenclature allows to directly identify the approximate chemical composition of the sample. The alkali metal dopants have been introduced as carbonates unless specified, as in the case of PdK4(Cl) and of PdK4(OH) where KCl and KOH have been used as K sources, respectively.

2.2. Characterization techniques

Micromeritics Autochem 2910 instrument was used for Temperature Programmed Reduction (TPR) and CO chemisorption measurements. TPR was carried out using a heating rate of 5 K min^{-1} from 193 to 873 K in a 5% H_2 in Ar mixture at a flow rate of 50 cm^3 min^{-1}. A molecular sieve trap was put between the sample holder and the detector in order to adsorb water eventually released from the sample.

CO chemisorption experiments were performed by the dynamic pulse method at 323 K. For catalysts calcined in air, a pre-reduction treatment at 393 K was performed. In order to determine the available surface Pd atoms (surface to volume ratio, S/V_{Chemi}) a CO/Pd average stoichiometry = 1 was assumed. This assumption was verified by a parallel series of measurements performed on three different samples treated at two different temperatures with H_2–O_2 static volumetric titration, which gave a O/Pd average stoichiometry close to 1 [31]. The two methods/techniques gave a CO/O ratio in the 0.94–1.13 range, which is a strong support for the assumption of a CO/Pd average stoichiometry = 1.

High-resolution transmission electron micrographs (HRTEM) were obtained with a JEOL 3010-UHR instrument operating at 300 kV, equipped with a 2 k × 2 k pixels Gatan US1000 CCD camera. Particle size distributions were obtained counting at least 200 particles. To present the data uniformly, a class width of 1 nm was chosen for all the particle size distributions. As the sample exhibited very small Pd particles, proper contrast/sampling conditions were set by: (a) counting only Pd particles found on regions of the support thin enough to appreciate the smallest contrast differences and (b) acquiring images at a magnification of 400 k × (0.026 nm per pixel). However, it must be considered that particles with diameter below 1 nm might escape the detection by this technique. For each particle size distribution the following values were estimated: (a) the average particle diameter, $\langle d\rangle_{TEM}$; (b) the standard deviation, σ; and (c) the surface to volume ratio, S/V_{TEM}, representing the overall Pd surface sites. We adopted a cubo-octahedral model to obtain the dispersion D (defined as the number of surface atoms over the total number of atoms in cluster) as a function of the cluster diameter d [32,33]. The d vs. D relationship was then applied not simply on the average $\langle d\rangle_{TEM}$ value, but weighted according to the particle size distribution obtained from the whole TEM analysis [30].

FTIR spectroscopy of adsorbed CO was performed on self-supported pellets inside an IR quartz cell suitable for thermal treatments in vacuum and/or controlled atmosphere. The samples were heated up to the desired reduction temperature under dynamical vacuum. The reduction process consisted in three subsequent H_2 dosages (equilibrium pressure P_{H2} = 120 Torr, 1 Torr = 133.3 Pa, contact time = 5 min). After the last H_2 removal at the reduction temperature down to $P_{H2} < 10^{-4}$ Torr, the samples were cooled down to 300 K in dynamical vacuum. This procedure allowed us to obtain the reduced sample in situ inside the IR cell. All the outgassed samples were then contacted in situ with CO (P_{CO} = 50 Torr). The FTIR spectra were recorded at room temperature at 2 cm^{-1} resolution, using a Bruker IFS28 spectrometer, equipped with a cryogenic MCT detector. P_{CO} was then gradually reduced in steps from 50 to 10^{-4} Torr. After each step, the FTIR spectrum of remaining adsorbed CO species was acquired. The final spectrum corresponded to CO species irreversibly adsorbed at 300 K. All the spectra reported in this work were normalized in order to take into account the different optical thickness of the samples, i.e the quantity of Pd crossed by the IR beam. Consequently, along the whole set of samples, the apparent intensity of a given band is directly proportional to the amount of carbonyl species responsible for the component so that all the spectra are directly comparable each other.

3. Results and discussion

3.1. Modification of the support during the doping process

We had demonstrated previously that the K-doping has great consequences on the morphology of the SA support [26] in terms of porous texture, surface area and chemical composition. The main results of that work, propedeutic to the present study, will be briefly summarized in the following. N_2 adsorption measurements and SEM microscopy demonstrated that the basic nature of the dopant solution causes the dissolution of the support (started already during the PdO deposition step), in a greater extent the higher the dopant concentration is. The dissolved material is not removed, but re-precipitates in the form of K silico-aluminate (hereafter K-SA) during the subsequent drying at 393 K. At higher temperature, the reaction between carbonate and support continues causing the mobilization of the support itself, with sintering phenomena that can reach the total collapse of the porous structure. It is expected that all these phenomena, besides having an important effect on the morphology and composition of the SA support, will also modify the accessibility and behaviour of the supported Pd particles, with important effects on their catalytic properties [26].

3.2. TPR results: the effect of K-doping on the Pd particles formation

TPR experiments are generally used to investigate the reducibility of the species present on a given support. By comparing the TPR results of undoped and doped samples it is possible to determine whether dopants have interacted already with the supported Pd^{2+} precursor (before or during reduction) or not. Moreover, the examination of the TPR profiles allows us to know which part of the catalyst is in the reduced state at a given temperature. This is of great relevance in understanding CO chemisorption and FTIR spectroscopy performed on samples reduced at different temperatures (vide infra Sections 3.3.2 and 3.4).

The TPR profiles for Pd_{und} and for the whole set of K-doped samples are shown in Fig. 1, while the quantitative hydrogen consumption (normalized to the sample weight) is reported in Table 1. The Pd_{und} sample (black curve in Fig. 1a) shows a single reduction peak starting at T_{start} = 276 K and terminating at 334 K (peak at T_{max} = 300 K). The integrated hydrogen consumption corresponds to a complete $Pd^{2+} \rightarrow Pd^0$ reduction: $H_{consumed}/Pd$ = 1.99, 2 being the theoretical value (see Table 1).

The addition of K does not affect the integrated area of the $Pd^{2+} \rightarrow Pd^0$ reduction peak, which is equivalent to a total reduction of all the Pd, independently from the concentration of the dopant (see Table 1). Notwithstanding this invariance, the presence of K affects the TPR profiles in many aspects (see Fig. 1a), as detailed in the following. (i) As the K loading increases, the main peak systematically shifts to higher temperature, by considering both T_{start} and T_{max} (see Table 1 and Fig. 1b), implying that the K-doping lowers the reducibility of Pd^{2+} species. The loading K/Pd = 1 defines two intervals: at lower values both T_{start} and T_{max} increase rapidly, while at higher values the phenomenon shows a much smaller slope (Fig. 1c). The behaviour up to K/Pd = 1 reflects a strong chemical interaction between potassium and Pd^{2+} species, which can eventually lead to the formation of a mixed compound already at low K content. In the following we will name this phase as KPdO, without referring to a precise stoichiometry. Indeed, it is well known that a very small amount of dopant is sufficient to strongly affect the reducibility of PdO [18]. A similar behaviour is observed also for mixed oxides, whose reducibility is modified upon small changes in composition [34–36]. (ii) With the exception of PdK0.2 (which is still similar to Pd_{und}), the other doped samples show a broadening of the TPR profiles (arbitrarily quantified by the $\Delta T = T_{start} - T_{end}$ value, see Table 1), which can be explained in terms of higher heterogeneity of species. The decrease of ΔT upon increasing the K loading can be due to a reduction of heterogeneity and/or to a faster kinetic when the $Pd^{2+} \rightarrow Pd^0$ reduction starts at higher T. (iii) Finally, the addition of K results in the appearance of a second reduction peak at much higher temperatures (in the 623–823 K interval, see Fig. 1a), which grows with the concentration of the dopant (Peak 2 in Table 1). As in most samples the hydrogen consumption related with this second peak exceeds the atomic H/K = 1 value (Table 1), it cannot be assigned to the direct $K^+ \rightarrow K^0$ reduction, but rather to a more complex reaction involving the reduction of the carbonate species. This hypothesis is supported by a parallel TPR experiment performed on a KCl-doped sample, exhibiting only the Pd reduction peak (data not reported for brevity). A similar explanation has been proposed to account for the presence of a high temperature TPR peak for Ca^{2+}-doped Pd–SiO_2 samples, in which $CaCO_3$ species decompose to CO_2, which is then hydrogenated over Pd to CH_4 [18].

From the reported data here, it is evident that a strong chemical interaction between K^+ ions and the supported Pd^{2+} precursor exists already at the lowest loadings. It is worth noticing that such a careful TPR analysis is possible only if the experiment starts far below RT in order to avoid Pd^{2+} reduction during stabilization of the baseline.

3.3. Pd particles size distribution and available Pd surface atoms: TEM vs. CO chemisorption

3.3.1. TEM

Fig. 2a reports the behaviour of the particle size distribution as a function of reduction temperature for the Pd_{und}, PdK4 and PdK20 samples (the last two chosen here as the intermediate and maximum K-loaded samples), as obtained by a systematic TEM analysis on a statistically significant number of particles. The $\langle d \rangle_{TEM}$ and the standard deviation (σ) for each distribution are reported in Table 2, together with the calculated S/V_{TEM} values that account for the particle size distribution [30]. A homogeneous distribution of the Pd particles on the support has been observed at any K loading and reduction temperature. A moderate sintering process occurs on the Pd_{und} sample upon increasing the H_2-reduction temperature, as evidenced by a change of the shape of the distribution, while no significant variation of $\langle d \rangle_{TEM}$ is observed.

Pd particles on PdK4 and PdK20 samples reduced at 393 K exhibit particle size distribution characterized by the same $\langle d \rangle_{TEM}$ and very similar σ as Pd_{und} reduced at the same temperature. This indicates that the presence of K does not affect either the dispersion or the particle size distribution of the metal phase. Since addition of K on the Pd_{und} occurs before reduction, this observation suggests that K-doping can change the chemistry of PdO particles (as evidenced by TPR measurements, vide supra Section 3.2), but not their dimension. Conversely, the increase of the reduction temperature from 393 K to 823 K results in a change of the particle size distribution (σ increases from 8 to 16 Å for PdK4, see Table 2), as for the Pd_{und}, but also in an increase of the mean particle size ($\langle d \rangle_{TEM}$ changes from 30 to 36 Å for PdK4). The change in the mean particle size is even more evident for higher K loadings ($\langle d \rangle_{TEM}$ increases from 27 to 37 Å for PdK20, see Table 2). The occurrence of a sintering process upon increasing the K loading and the reduction temperature is confirmed by the calculated S/V_{TEM} values (see Table 2).

Besides the effect on the dimension of the particles, K-doping has a second effect. On PdK4 and PdK20 samples, most of the particles appeared "covered" by a coating 1–2 nm thick (see Fig. 2b); the effect is more pronounced at high doping levels and high reduction temperatures. This phase, never observed in the case of the undoped samples and thus surely associated with the addition

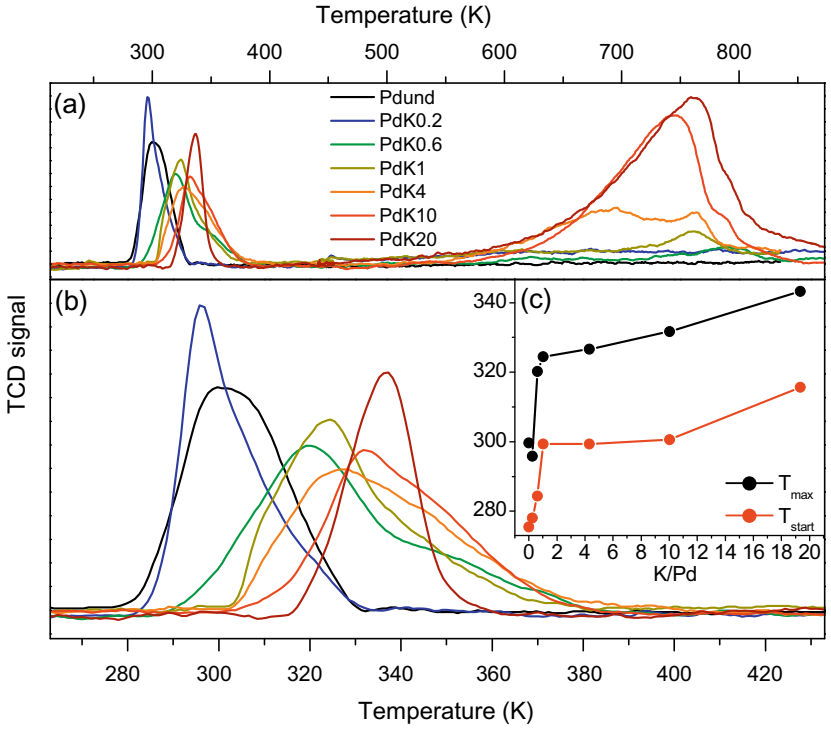

Fig. 1. (a) TPR curves of Pd_{und} and of the whole set of K-doped Pd/SiO_2–Al_2O_3 samples in the 253 to 823 K interval (see legend for the K/Pd atomic ratio). (b) Magnification of the region 263–433 K, corresponding to the $Pd^{2+} \rightarrow Pd^0$ reduction. (c) Values of the temperatures corresponding to the beginning of the reduction (T_{start}) and to the maximum of the reduction peak (T_{max}) as a function of the K/Pd atomic ratio.

Table 1
Summary of the quantitative data extracted from the TPR experiments reported in Fig. 1b. The theoretical total Pd reduction corresponds to atomic ratios of $H_{consumed}/Pd = 2$. Peak 1 and peak 2 correspond to reduction of Pd^{2+} species and of carbonates, respectively.

Sample	Peak 1				Peak 2	
	T_{start} (K)[a]	T_{max} (K)	ΔT (K)[b]	$H_{consumed}/Pd$ (atomic ratio)	$H_{consumed}/Pd$ (atomic ratio)	$H_{consumed}/K$ (atomic ratio)
Pd_{und}	276	300	59	1.99	0.0	0.0
PdK0.2	278	296	56	2.04	0.0	0.0
PdK0.6	284	320	100	2.24	0.9	1.6
PdK1	299	324	81	2.02	1.4	1.4
PdK4	299	327	82	2.07	5.4	1.3
PdK10	301	332	85	1.94	10.9	1.1
PdK20	316	343	50	1.86	15.2	0.8

[a] T_{start} is defined as the temperature where the first derivative of the TCD signal exceeds the arbitrary value of 5×10^{-4} TCD signal K^{-1}.
[b] $\Delta T = T_{end} - T_{start}$, being T_{end} defined as the temperature where the absolute value of the first derivative of the TCD signal becomes smaller than 5×10^{-4} TCD signal K^{-1}.

of K_2CO_3, is characterized by interference fringes, suggesting a crystalline nature. Washing of the sample does not remove the covering phase (see Fig. 2c), indicating that it is constituted by an insoluble matter, like the support mobilized and re-precipitated during the doping process and sintered during the reduction step [26]. The weak contrast of the interference fringes and the instability of this phase under the electron beam prevented the acquisition of high-resolution images with the sufficient quality needed to identify the phase via *d*-spacing measurement. Moreover, this instability forced us to work with a highly dispersed beam, i.e. in conditions not suitable to localize impurities by EDX analysis. However, its instability suggests that the covering phase is constituted by a relatively low-melting material, in agreement with the hypothesis already advanced by us of the formation of low-melting K salts during the doping procedure [26].

3.3.2. CO chemisorption

Complementary and additional information on the particle size distribution and on the presence of a covering phase can be obtained by CO chemisorption experiments. The true available Pd surface atoms (S/V_{Chemi}) of Pd_{und}, PdK4 and PdK20 samples at the three different reduction temperatures are reported in Table 2, and compared with the potentially available Pd surface atoms (S/V_{TEM}), as obtained by TEM. $S/V_{Chemi} \approx S/V_{TEM}$ for Pd_{und} H_2-reduced at 393 K, demonstrating that the cubo-octahedral model and the fraction of Pd surface in interaction with the support adopted to convert the particle-size distribution into S/V_{TEM} and the 1:1 CO/Pd stoichiometry used to analyze the chemisorption data are correct assumptions. For all the samples $S/V_{Chemi} < S/V_{TEM}$, and the difference is greater the high the K loading is and the high the reduction temperature is. This loss of dispersion measured by CO chemisorption can be explained both by considering an important poisoning of the potentially available Pd surface and/or by taking into account the presence of a phase covering the Pd particles (as observed by TEM). However, it is important to notice that with most of the particles being completely covered by a crust on the high K-loaded samples at least a fraction of the covering phase should be permeable to CO molecules in order to justify S/V_{Chemi} values sufficiently different from zero. This point will have an important relevance in the discussion of the FTIR spectra (see Section 3.4).

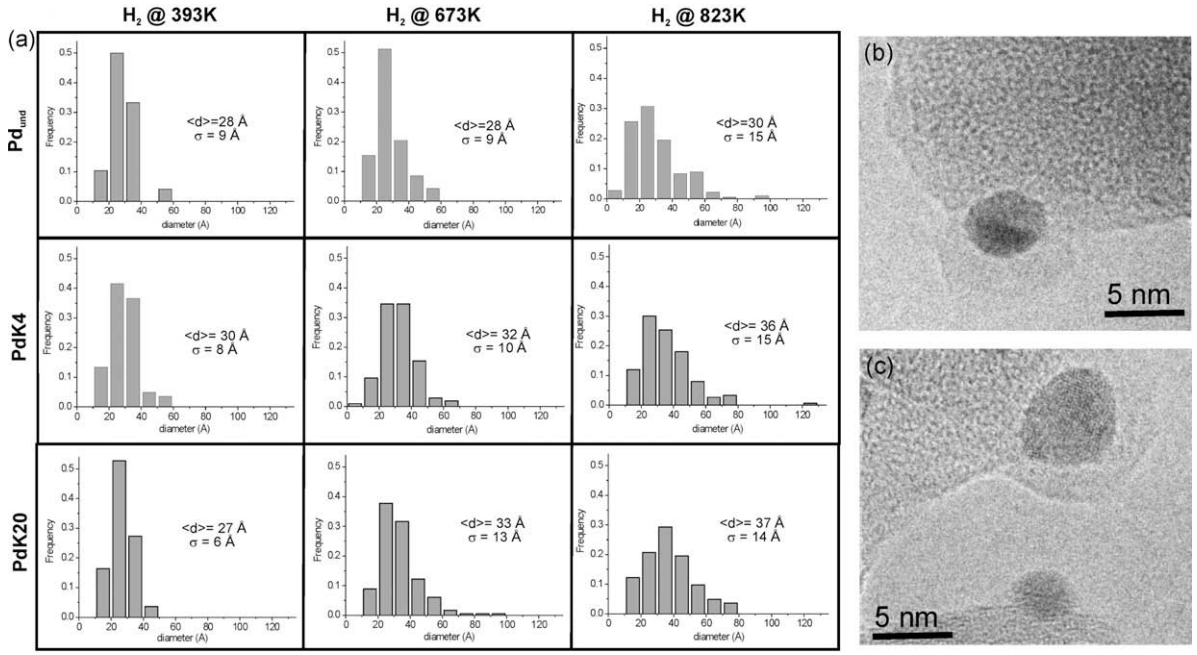

Fig. 2. Part (a): particle size distribution on the Pd_{und}, PdK4 and PdK20 samples H_2-reduced at 393, 673 and 823 K. Part (b) shows a high-resolution transmission electron micrograph of the PdK20 sample reduced in H_2 at 673 K, showing the typical particle covering observed for most of the doped samples. Part (c): the same sample subjected to a washing procedure (see Experimental Section), still showing the same covering phase.

Table 2
Mean particle size ($\langle d\rangle_{TEM}$), standard deviation (σ_{TEM}) and surface/volume atoms ratio (S/V_{TEM}) as obtained by TEM, compared to the surface/volume atoms ratio as obtained by CO chemisorption (S/V_{Chemi}), for Pd_{und}, PdK4 and PdK20 samples, as a function of the H_2-reduction temperature.

T (K)	K/Pd = 0				K/Pd = 4				K/Pd = 20			
	$\langle d\rangle_{TEM}$ (Å)	σ_{TEM} (Å)	S/V_{TEM} (%)	S/V_{Chemi} (%)	$\langle d\rangle_{TEM}$ (Å)	σ_{TEM} (Å)	S/V_{TEM} (%)	S/V_{Chemi} (%)	$\langle d\rangle_{TEM}$ (Å)	σ_{TEM} (Å)	S/V_{TEM} (%)	$S/VS/V_{Chemi}$ (%)
393	28	9	29	28	30	8	29	26	27	6	33	22
673	28	9	29	21	32	10	26	19	33	13	23	16
823	30	15	24	12	36	15	21	16	37	14	21	7

In order to further investigate the reason why a gradual loss of dispersion is observed upon increasing K loading and reduction temperature, CO chemisorption experiments have been extended to the entire sequence of the samples that have been subjected to thermal treatments at increasing temperature both in H_2 and in air. The S/V_{Chemi} curve vs. K/Pd concentration obtained for the entire set of data is reported in Fig. 3. These data will be discussed in the following by separating the effect of the treatment atmosphere.

Doped samples calcined in air at increasing temperature

Starting with the samples treated at 393 K (Fig. 3a, black curve), the S/V_{Chemi} curve shows a maximum at K/Pd = 0.6, an evidence that two distinct processes in direct mutual competition occur on the sample. The first process, at low K/Pd ratio, causes a small but significant increase of dispersion with respect to Pd_{und}. The phenomenon can be due to: (i) a bulk modification of PdO particles that, consequently to interaction with K, give PdO crystals different in size, shape or smoothness; (ii) a removal of possible decorations formed by carrier during impregnation (the basic solutions used for Pd deposition-precipitation are aggressive towards the support [26]). The second process, at high K/Pd ratio, causes an apparent decrease of Pd dispersion, which can be explained in terms of partial coverage of Pd surface, as shown by TEM analysis (see Fig. 2b). TEM measurements on washed PdK20 sample indicated that the encapsulating phase is composed by insoluble matter coming from the support mobilized during the doping step. This is confirmed by S/V_{Chemi} value on the washed PdK20, showing only a partial recovery of "disappeared" surface (black star in Fig. 3a). In particular, upon washing the dispersion increases from 21.9% to 24.6%, while the dispersion of Pd_{und} sample is 28.2% and the maximum dispersion achieved on doped samples is 30.2% (for PdK0.6 sample). Notice that the insoluble covering should not be regarded as a mere physical covering because the washed sample shows FTIR spectra of adsorbed CO different from those found on Pd_{und} sample (vide infra Section 3.4). Finally, a similar dispersion is observed when Pd/SA is doped by KOH (see empty square in Fig. 3a), confirming the role of the basic doping solution in affecting the available Pd surface sites.

Heating at 673 K in air (Fig. 3a, blue curve) causes changes similar to those observed after treatment at 393 K. Conversely, upon heating at 823 K in air (Fig. 3a, red curve) a relevant loss of dispersion is observed, especially for high K/Pd ratio (S/V_{Chemi} = 10.4% for PdK20). TEM does not reveal a significant Pd sintering, and thus the best candidate to explain this behaviour is again the mobility of the support (see Section 3.1). In particular, N_2 adsorption measurements demonstrated that the greater the modification of the support is (in terms of decrease in surface area), the greater is the loss of dispersion shown by Pd particles [26].

Doped samples H_2-reduced at increasing temperature

The effect of thermal treatments in H_2 (Fig. 3b) is different from what is observed in air (Fig. 3a). The S/V_{Chemi} curve as a function of K/Pd ratio for the samples reduced at 673 K (Fig. 3b, blue curve) presents the same shape as that obtained for the samples reduced at 393 K (Fig. 3b, black curve). An increase of dispersion is observed

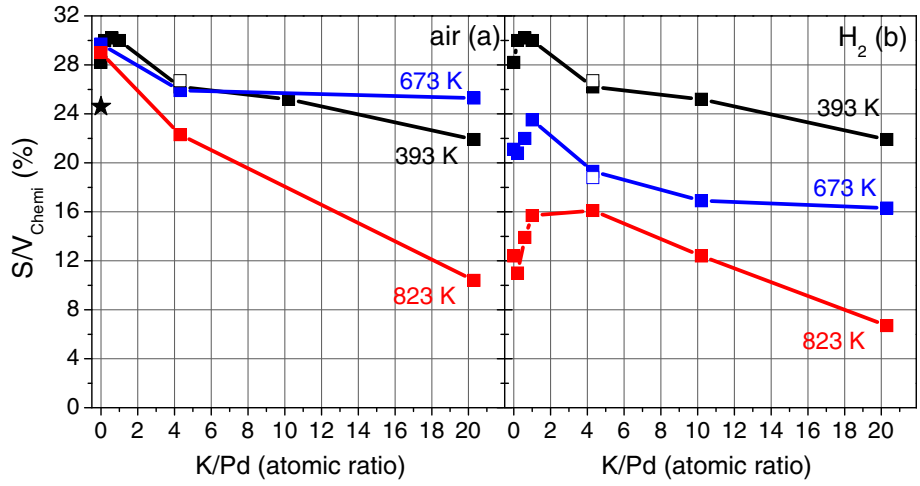

Fig. 3. Surface/volume atoms ratio as obtained by CO chemisorption (S/V_{Chemi}) for Pd_{und} and the entire sequence of doped samples, treated at 393 K (black), 673 K (blue), or 823 K (red), either in air (part a) or in H_2 (part b) atmosphere, as a function of the K/Pd ratio. The black star represents the S/V_{Chemi} value for the PdK20 sample treated at 393 K after the washing procedure. Empty squares represent the S/V_{Chemi} value for the PdK4(OH) sample. Note that the samples treated at 393 K can be considered as a part of both series because the CO chemisorption measurements imply a H_2 pre-reduction of the sample at 393 K. (For interpretation of the references in colour in this figure legend, the reader is referred to the web version of this article.)

at low K/Pd ratio with a maximum shifted from K/Pd = 0.6 to K/Pd = 1.0, followed by a decrease between K/Pd = 1.0 and K/Pd = 4.3. However, in the case of samples reduced at 673 K, the measured dispersion is lower than that measured on samples calcined at the same temperature by about 30%. As has been discussed already in the case of reduction at 393 K, the effect of doping by KOH is almost the same as that observed for K_2CO_3-doping (see empty squares in Fig. 3b).

At 823 K (Fig. 3b, red curve), the trend is roughly similar, but i) the maximum is further shifted above K/Pd = 1.0, and ii) for K/Pd > 4.3 the dispersion decreases monotonously with K/Pd ratio. The greatest difference with respect to the trend observed at lower temperature occurs for Pd_{und} and for the doped samples at low K loading. All the processes examined to explain the loss of Pd dispersion observed in the case of samples calcined in air account only for a fraction of decrease of accessible surface sites, and a new process must be invoked to account for the dramatic loss of dispersion measured by CO chemisorption. The more reasonable hypothesis to justify the experimental data is an important poisoning of the potentially available Pd surface during high temperature H_2-reduction process, which is mostly effective at low K loadings. Note that the loss of dispersion due to poisoning, roughly evaluated by the difference in S/V_{Chemi} values between calcined and reduced samples at 823 K is 17%, 6% and 4% for Pd_{und}, PdK4 and PK20, respectively. However, CO chemisorption is not informative on the nature of poisoning species, and more details will be given by FTIR of adsorbed CO (see Section 3.4.).

3.4. Characterization of accessible surface sites by FTIR of adsorbed CO

TPR experiments (vide supra Section 3.2), monitoring the formation of Pd particles along the H_2 reduction process, told us that the dopant phase has already interacted with the precursor Pd^{2+} phase. The question is now if this interaction is still holding on the reduced Pd metal particles. TEM and CO chemisorption (vide supra Section 3.3) indicate that both the K-doping and the reduction temperature have a profound influence in determining the true dispersion of the Pd particles. However, none of the examined techniques give details on the quality of the accessible surface sites. In order to verify whether K still interacts with the reduced Pd particles and to understand in which way, we probed the surface of Pd particles by means of FTIR spectroscopy of adsorbed CO, which is an efficient technique to obtain information on the exposed faces and on their defectivity [37–45]. It is worth noticing that among all the applied techniques FTIR of adsorbed CO is the only one with the sufficient sensitivity to determine, even if in an indirect way, the nature of the poisoning species at the Pd surface.

3.4.1. Doped samples reduced at 393 K

The FTIR spectra of CO adsorbed at 300 K on Pd_{und} and on the doped samples reduced at 393 K are reported in Fig. 4a–e, upon decreasing coverage (θ). The spectra of Pd_{und} are characterized by three main components that are assigned, from high to low $\tilde{\nu}$(CO), to: (i) linear carbonyls on Pd(1 1 1) faces and/or on defects (band I); (ii) two-fold bridged carbonyls on Pd(1 0 0) faces (band II) and (iii) two-fold bridged carbonyls on Pd(1 1 1) faces (band III) [37,40,46–62]. The progressive increase of K content causes a gradual modification of the CO spectra (Fig. 4a–e). Already at low K/Pd ratios, the spectra of adsorbed CO are different with respect to those obtained for the Pd_{und} system, suggesting that the dopant phase has interacted with the reduced Pd metal particles already at low K loadings. In other words, K interacts not only with the Pd^{2+} precursor (see TPR data, Section 3.2), but this interaction still holds once the Pd^{2+} precursor is reduced into Pd metal particles.

The changes in CO spectra upon increasing the K loading can be rationalized in two main phenomena. (1) A progressive decrease of the intensity of bands I and II with respect to the Pd_{und} system (part a), and a simultaneous increase of band III. At the highest K loadings the spectra are dominated by this last band, which is quite sharp and intense. (2) The change in intensity is accompanied by a general downward shift of all the components: as an example, band I undergoes a shift of $\Delta\tilde{\nu} = -20\ cm^{-1}$ (from 2087 cm^{-1} in Pd_{und} to 2067 cm^{-1} in PdK20, values taken at θ_{max}), whereas band III undergoes a downward shift of $\Delta\tilde{\nu} = -64\ cm^{-1}$ (from 1930 cm^{-1} in Pd_{und} to 1866 cm^{-1} in PdK20, values taken at θ_{max}).

Spectra similar to those obtained at high K loadings (K/Pd $\geqslant$ 4) are reported in the literature by Liotta et al. [24,63] for Na^+-doped Pd/SiO_2 samples. The dominant component at very low frequency was attributed by the authors to a Pd–CO–Na^+ species, according to the well-documented effect in coordination chemistry of a downward shift of $\tilde{\nu}$(CO) when a Lewis acid, such as an alkali ion,

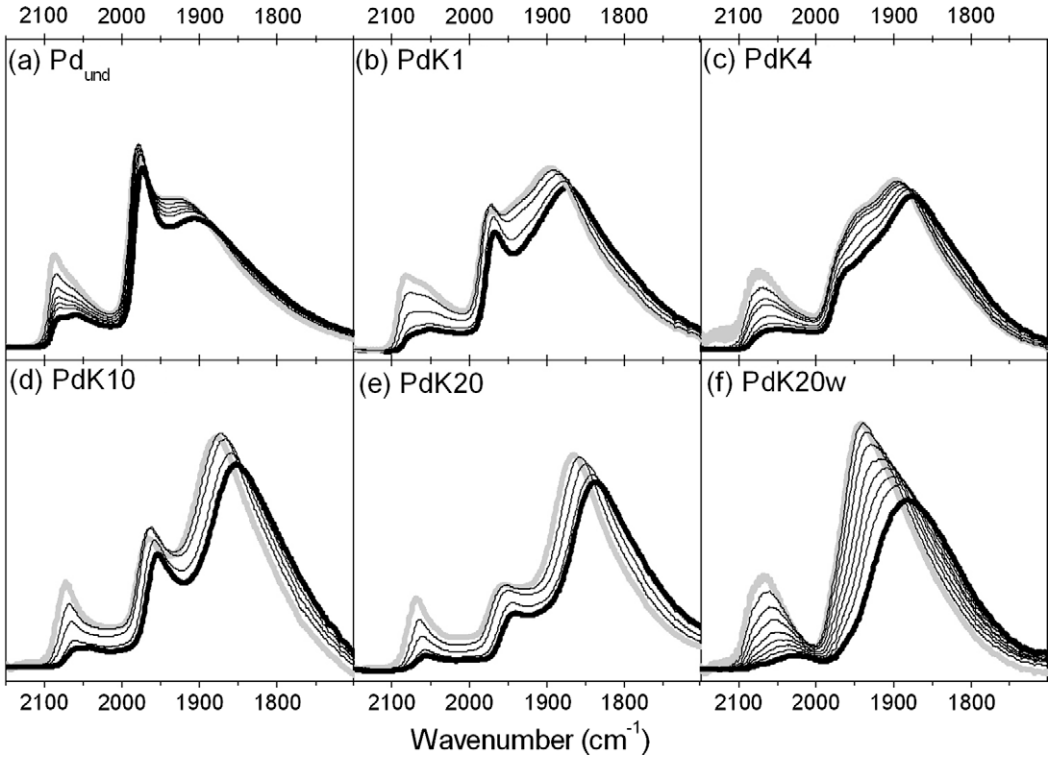

Fig. 4. FTIR spectra of CO dosed at RT on Pd_{und} (part a) and on Pd/SA samples (parts b–e) doped with increasing amount of K, previously reduced at 393 K. The sequences of spectra show the effect decreasing P_{CO}, from 50 (grey curve) to 10^{-4} Torr (bold black curve). Part (f) shows the same experiment performed on the PdK20 sample after washing.

interacts with the oxygen of the carbonyl ligand in metal carbonyl complexes, with the consequent weakening of the C–O bond [64–66]. Similar low frequency bands are also reported for alkali-promoted Ni/SiO_2 [67] and Pd/SiO_2 [18,68,69] catalysts. This assignment also explains the fact that when the Na^+ promoter is added to the Pd/SiO_2 catalyst, the bridging/linear carbonyl ratio increases (from 0.92 to 4.01 when Na/Pd = 0.4); in fact, Na^+ addition produces per se an increase of the bridging/linear ratio, which can be explained by an evolution of the linear species into the Pd–CO–Na^+ ones [24,63].

Following this interpretation to explain the gradual growth of the relevant band at very low $\tilde{\nu}$(CO) values, the question is the chemical state of potassium. From the results discussed until now, we know that two phenomena are contemporaneously present: (i) the K coming from the KPdO phase formed on the PdO particles during the doping step (yellow symbol in Fig. 6) is still present after H_2 reduction at 393 K, maybe in the form of K-oxide/hydroxide (red symbol in Fig. 6), as no sign of reduction of K is present; (ii) the Pd particles are, at least partially, covered by an encapsulating phase (observed by TEM, Fig. 2b) mainly due to the support, which is solubilized and re-precipitated during the doping step. Both phenomena should have not only a physical effect, but also a chemical effect. It is worth noticing that very similar spectra are obtained for the PdK4(OH) sample (not reported for brevity), which is in agreement with the CO chemisorption results.

In order to separate the role played by the K/oxide-hydroxide phase from that played by the insoluble encapsulating phase in defining the FTIR features of adsorbed CO, the PdK20 sample was subjected to a careful washing procedure. This treatment should remove only the species soluble in H_2O, such as the K^+ species on the PdO phase and the unmodified carbonate, whereas eventual insoluble species (such as the K–SA phase or support material re-precipitated after impregnation [26]) remain on the surface. Therefore, we expect that the spectra of adsorbed CO should change with respect to the un-washed case, but they should remain different from the Pd_{und} ones because the insoluble crust remains. After the washing procedure, no bands in the carbonate region are evident (spectra not reported for brevity). The spectra of adsorbed CO (reported in Fig. 4f) are no more characterized by the anomalous low frequency component dominating the spectra of the sample before washing (Fig. 4e), which is in agreement with its assignment to carbonyls perturbed by the proximity of K^+ cations. Therefore, we can conclude that the washing procedure removes the main component responsible for the anomalous position of band III, which must be a soluble phase. However, even if the low frequency component shifts again to "standard" values, the spectra are still different from those obtained on Pd_{und} (Fig. 4a). In particular, component II seems to be totally absent, indicating that the (100) faces are completely inaccessible to the CO probe molecules. This suggests that the washing procedure if from one side removes the KPdO phase formed on the PdO particles during the doping stage, from the other side it acts as a covering procedure (both PdO and the SA are again dissolved into the basic solution and re-precipitate a second time, so that the PdO particles are covered two times) [26]. This new covering effect is more active towards the (100) faces. These results are in agreement with CO chemisorption data (black star in Fig. 3a), showing that only a small fraction of the dispersion is recovered after washing, and is supported by TEM measurements (see Fig. 2c), showing that most of the particles are still covered by a crust (necessarily of something insoluble, like the support material).

3.4.2. Doped samples reduced at 673 and 823 K

While the FTIR spectra of CO adsorbed on the samples pre-reduced at 393 K are strongly modified upon increasing the K loading (Fig. 4b–e), on the samples pre-reduced at 673 K (see Fig. 5a–c) and

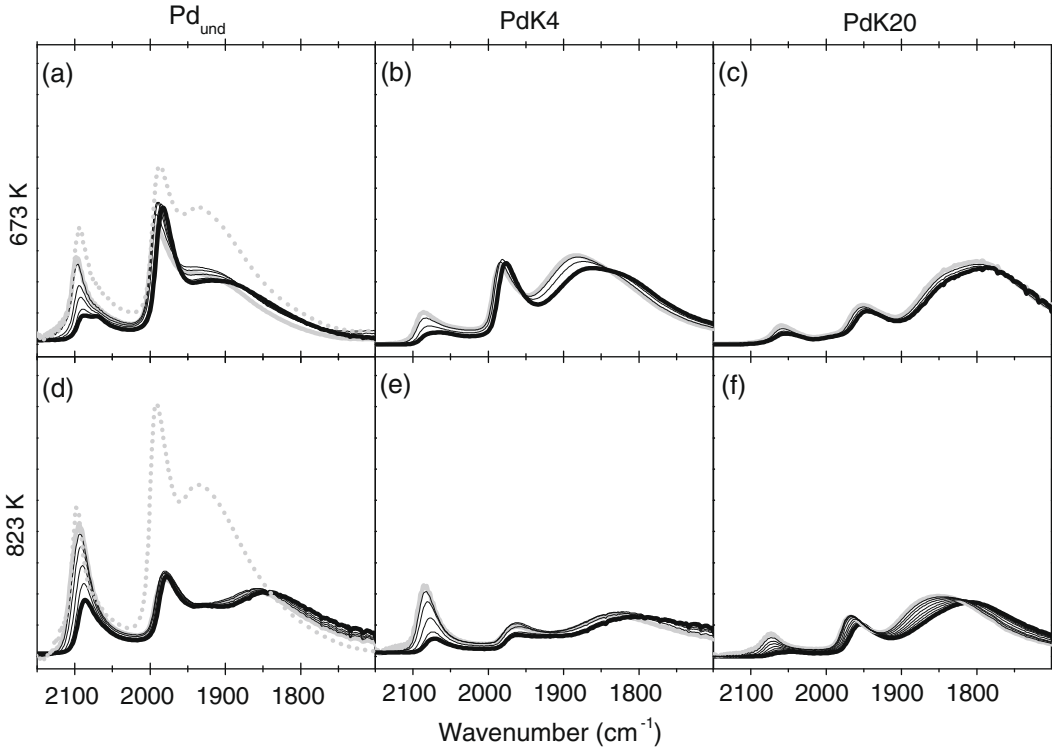

Fig. 5. FTIR spectra of CO dosed at RT on Pd_{und} (parts a,d), PdK4 (parts b,e) and PdK20 samples (parts c,f) previously reduced at 673 and 823 K. The sequences of spectra show the effect of decreasing P_{CO}, from 50 (grey curve) to 10^{-4} Torr (bold black curve). Dotted spectra in parts (a) and (d) are the highest CO coverage on Pd particles obtained by thermal decomposition of PdO at 673 and 823 K, respectively.

823 K (see Fig. 5d–f) the effect of the K-doping is less evident. Fig. 5 reports the spectra in the case of Pd_{und}, PdK4 and PdK20 samples, whereas those obtained on sample with intermediate K loadings have been omitted for simplicity, having a similar behaviour.

Starting with the Pd_{und} sample, the following changes occur upon increasing the reduction temperature up to 823 K (Fig. 5a,d): (i) band II decreases in intensity; (ii) the relative ratio between band I and band III is reversed and (iii) an important red-shift of band III is observed. TEM measurements do not evidence a change in the shape of the Pd particles. Moreover, these spectral modifications are observed only when thermal treatment is performed in the presence of H_2 while when the thermal treatment is performed in vacuo, IR spectroscopy of CO results in spectra very close to those obtained for the Pd_{und} sample H_2-reduced at 393 K (compare the dotted spectra in Fig. 5a,d with the highest coverage spectrum in Fig. 4a; note that these spectra imply that PdO has decomposed into Pd metal already at 673 K in vacuo) [30]. These observations suggest that poisoning species are present in the support, and that they are extracted only in the presence of H_2, which is in agreement with the hypothesis that has already been advanced to explain the CO chemisorption experiments. The poisoning species (having a molecular character) should occupy the same sites of a bridged CO molecule, so that the incoming CO molecules arrange themselves preferentially in a linear way. This interpretation also explains the red-shift of band III because the poisoning of the exposed adsorption sites does not allow the coupling of the CO oscillators to be fully operative [44].

Among the possibilities we have identified three candidates, all present in the support as impurities or arising from raw materials: S, Cl and Ca. Sulphur is the best candidate because (i) it is a well-known poison of noble metals [70–76], (ii) it is present as "inert" sulphate in the support, which is reduced by H_2 to poisonous H_2S (in air the process does not occur) and (iii) very small amounts of S are sufficient to significantly poison Pd surface (0.2 wt.% is sufficient to form a surface stoichiometry $S/Pd_{surf} = 1/1$, but a much lower ratio is sufficient to change the Pd surface deeply). Chlorine, a residual presence that arises from Pd raw material or is already present as an impurity in the carrier, is a known poison similar to S [76]. However, the release from the carrier to Pd does not require the presence of H_2 because it is already in the reduced state. Calcium poisoning has been claimed by Prins et al. [18], but here this choice is not able to explain the determining effect of H_2 and the differences observed by FTIR spectroscopy between "poisoned" undoped samples and K-doped samples (see discussion here below).

Coming to the doped samples, the CO spectra on systems reduced at 673 K (Fig. 5b and c) are characterized by the typical three components observed in the case of the Pd_{und} system (Fig. 5a). This suggests that the species responsible for the "anomalous" spectra observed on the sample pre-reduced at 393 K starting from K/Pd > 4 (intense and sharp component at low frequencies) are now (at least partially) removed. In more detail, components I and II appear at frequencies higher with respect to the corresponding ones in the case of the same sample pre-reduced at 393 K, indicating that a larger portion of the exposed surfaces is clean (better coupling of the CO oscillators [44,77]), while an opposite behaviour is shown by component III. This complex evolution should be ascribed to the strong modifications induced on the entire sample upon increasing the reduction temperature [26]. On the samples pre-reduced at 823 K (Fig. 5e and f), a further evolution of the FTIR spectra is observed upon increasing the K loading. The PdK4 sample is still characterized by an anomalous inversion of the relative intensity of the three components, and in particular by an increase of band I with respect to the other components, in a similar way to what is observed in the case of the Pd_{und} system (Fig. 5d). Conversely, the PdK20 sample shows the usual spectra expected in the case of Pd particles exhibiting (111) and (100) faces, with the three components lying at almost the same frequencies

observed for the sample pre-reduced at 673 K and the same relative intensity ratio. In this case the shift of the bands upon decreasing θ is, however, greater that on the sample pre-reduced at 673 K, indicating a greater coupling of the CO oscillators and thus larger exposed surfaces. All these results suggest that the presence of a high K loading inhibits the poisoning of the Pd particles by the species extracted from the support (most probably S) at 823 K in the presence of H_2. Note that PdK4 sample is still poisoned, even if in a lower extent with respect to Pd_{und} system. Finally, the lower global intensity of the spectra is easily explained in terms of increasing sintering and modification of the support (growth of the SA particles), with both phenomena being promoted by the presence of the high K content.

4. Conclusions

In this work, all the processes occurring on a Pd/SA system doped with K_2CO_3 as a function of (i) the doping loading (in the 0.25–20.3 K/Pd atomic ratio interval), (ii) the activation temperature and (iii) the activation atmosphere (air or H_2) have been investigated by means of several complementary techniques (TPR, TEM, CO chemisorption and FTIR spectroscopy). In particular, attention was focused on the effects of all these variables on the reducibility, sintering and surface properties of Pd metal nanoparticles. All the modifications involving the Pd/SA sample during the doping process and the subsequent H_2-reduction at increasing temperatures are schematically represented in Fig. 6, and can be summarized as follows.

(i) Potassium doping has a great influence on the starting Pd^{2+} precursor phase (orange particles in Fig. 6), already at the lowest loadings. TPR data indicate that there exists a strong chemical interaction between potassium and Pd^{2+} species, lowering their reducibility. The presence of a mixed KPdO compound (small yellow spheres in Fig. 6) is advanced.

(ii) Even if potassium doping changes the chemistry of PdO particles, it does not affect either the dispersion or the distribution of the metal phase (grey particles in Fig. 6). However, at high reduction temperature, the presence of potassium causes the occurrence of a moderate sintering process.

(iii) Both the potassium doping and the reduction temperature have a profound influence in determining the fraction of truly available Pd surface sites; in particular, the higher are the potassium loadings and the reduction temperature, the higher is the fraction of the Pd particles not available to probe molecules. The lost of accessible Pd surface can be explained both in terms of (a) covering by an encapsulating phase coming from the support mobilized during the doping step (light green in Fig. 6), and (b) poisoning by a K-oxide/hydroxide phase (small red spheres in Fig. 6) derived from the original mixed KPdO compound.

(iv) Conversely, the presence of the dopant inhibits the poisoning of the Pd surface by sulphur (small black spheres in Fig. 6) released from the support in the undoped sample during the thermal treatments in H_2 atmosphere.

(v) Finally, the atmosphere in which the treatments are conducted is determinant in favouring some of these processes. The most relevant difference concerns the poisoning of the Pd particles by sulphur released from the support, which occurs in the presence of H_2 and not in air. Generally speaking, which atmosphere is more advantageous for the catalytic properties is difficult to say, and depends on the kind of reaction. Usually a "clean" catalyst presents a higher activity with respect to a "poisoned" one, but sometimes is

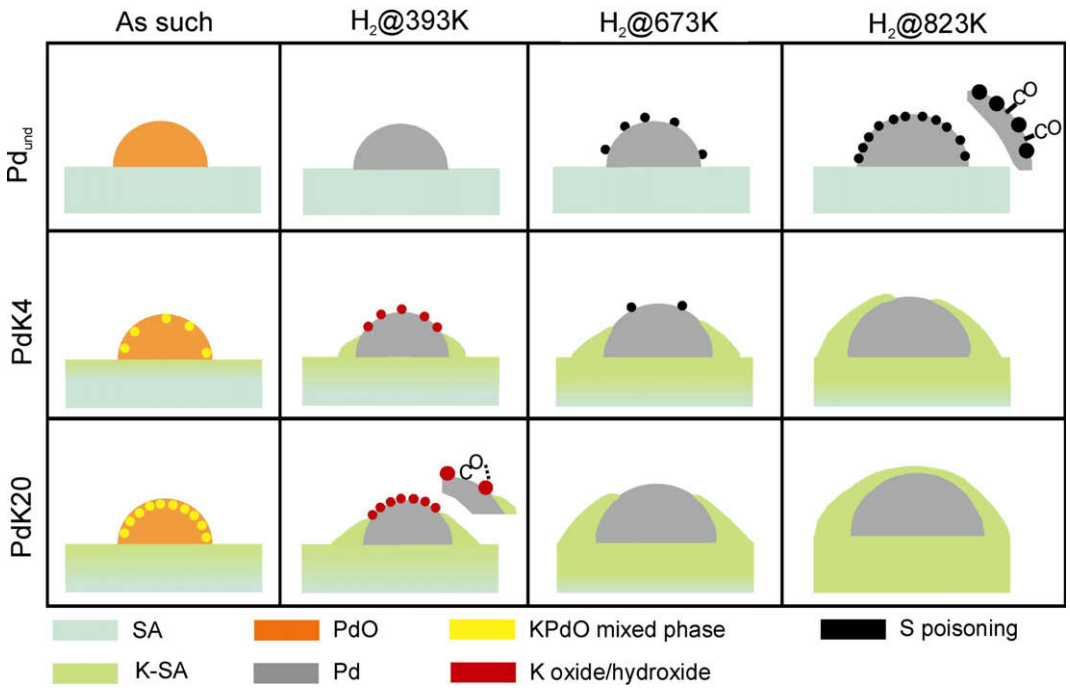

Fig. 6. Schematic representation of all the modifications involving Pd/SA sample during the doping process (with K_2CO_3) and the subsequent H_2-reduction at increasing temperatures. The picture reports a section view around a single particle, which is represented as a semi-sphere for simplicity (i.e. without taking into account the presence of the different faces expected in the case of a cubo-octahedral model). PdO and Pd particles are represented with orange and grey colours, respectively, with an increasing dimension qualitatively in agreement with the TEM observation. The SA support is represented with light blue colour, while its modification upon K insertion is in light green. Small black spheres schematically represent the presence of sulphur poisoning. Small yellow spheres represent the formation of a KPdO mixed phase, which evolves into K oxide/hydroxide (small red spheres) on metal Pd particles. The insets show a detail on the CO interaction with Pd particles. (For interpretation of the references in colour in this figure legend, the reader is referred to the web version of this article.)

less selective. In these cases a poisoning/doping process could be beneficial for the selectivity, even if it causes a loss in activity.

As a final conclusion, it is worth noticing that most of the processes described in the case of the Pd/SA sample during the doping process and the subsequent treatments can be present on different catalytic systems characterized by other metal particles and doped by other alkali-metals. This work definitely demonstrates that the application of a limited number of characterization techniques can be misleading and only the application of several techniques gives a comprehensive picture of all the phenomena characterizing a real catalytic system.

Acknowledgment

We are indebted to Massimo Graziani (Chimet S.p.A.) for the CO chemisorption measurements.

References

[1] P.N. Rylander, in: Catalytic Hydrogenation in Organic Syntheses, Academic Press, Inc., New York, 1979.
[2] H.U. Blaser, A. Indolese, A. Schnyder, H. Steiner, M. Studer, J. Mol. Catal. A – Chem. 173 (2001) 3.
[3] A. Zecchina, E. Groppo, S. Bordiga, Chem. – Eur. J. 13 (2007) 2440.
[4] L. Guczi, Catal. Today 101 (2005) 53.
[5] A.M. Venezia, L.F. Liotta, G. Pantaleo, V. La Parola, G. Deganello, A. Beck, Z. Koppany, K. Frey, D. Horvath, L. Guczi, Appl. Catal. A – Gen. 251 (2003) 359.
[6] A.M. Venezia, V. La Parola, B. Pawelec, J.L.G. Fierro, Appl. Catal. A – Gen. 264 (2004) 43.
[7] S. Murata, K. Aika, J. Catal. 136 (1992) 110.
[8] S. Murata, K. Aika, J. Catal. 136 (1992) 118.
[9] H. Pinxt, B.F.M. Kuster, G.B. Marin, Appl. Catal. A – Gen. 191 (2000) 45.
[10] V. Ponec, Appl. Catal. A 149 (1997) 27.
[11] L. Bollmann, J.L. Ratts, A.M. Joshi, W.D. Williams, J. Pazmino, Y.V. Joshi, J.T. Miller, A.J. Kropf, W.N. Delgass, F.H. Ribeiro, J. Catal. 257 (2008) 43.
[12] G. Neri, A.M. Visco, A. Donato, C. Milone, M. Malentacchi, G. Gubitosa, Appl. Catal. A 110 (1994) 49.
[13] S. Scire, C. Crisafulli, R. Maggiore, S. Minico, S. Galvagno, Appl. Surf. Sci. 93 (1996) 309.
[14] S. Scirè, S. Minicò, C. Crisafulli, Appl. Catal. A 235 (2002) 21.
[15] N. Mahata, K.V. Raghavan, V. Vishwanathan, Appl. Catal. A 182 (1999) 183.
[16] Y.H. Park, G.L. Price, Ind. Eng. Chem. Res. 31 (1992) 469.
[17] D. Teschner, E. Vass, M. Hävecker, S. Zafeiratos, P. Schnörch, H. Sauer, A. Knop-Gericke, R. Schlögl, M. Chamam, A. Wootsch, A.S. Canning, J.J. Gamman, S.D. Jackson, J. McGregor, L.F. Gladden, J. Catal. 242 (2006) 26.
[18] A.F. Gusovius, T.C. Watling, R. Prins, Appl. Catal. A – Gen. 188 (1999) 187.
[19] A.F. Gusovius, R. Prins, J. Catal. 211 (2002) 273.
[20] A.M. Kazi, B. Chen, J.G. Goodwin, G. Marcelin, N. Rodriguez, T.K. Baker, J. Catal. 157 (1995) 1.
[21] A.N. Pestryakov, V.V. Lunin, S. Fuentes, N. Bogdanchikova, A. Barrera, Chem. Phys. Lett. 367 (2003) 102.
[22] R.B. Anderson, in: P.H. Emmet (Ed.), Catalysis, Vol. IV, Reinhold, New York, 1956, pp. 1–5.
[23] W.D. Mross, Catal. Rev. Sci. Eng. 25 (1983) 591.
[24] L.F. Liotta, G.A. Martin, G. Deganello, J. Catal. 164 (1996) 322.
[25] D. Duca, F. Arena, A. Parmaliana, G. Deganello, Appl. Catal. A 172 (1998) 207.
[26] R. Pellegrini, G. Leofanti, G. Agostini, E. Groppo, M. Rivallan, C. Lamberti, Langmuir 25 (2009) 6476.
[27] R. Berthoud, P. Délichère, D. Gajan, W. Lukens, K. Pelzer, J.-M. Basset, J.-P. Candy, C. Copéret, J. Catal. 260 (2008) 387.
[28] J.W. Geus, A.J. van Dillen, in: K.H. Ertl, G.J. Weitkamp (Eds.), Handbook of Heterogeneous Catalysis, vol. 1, Wiley-VCH, Weinheim, 1997.
[29] P.A. Simonov, V.A. Likholobov, in: A. Wieckowski, E.R. Savinova, C.G. Vayenas (Eds.), Catalysis and Electrocatalysis at Nanoparticle Surfaces, Marcel Dekker Inc., 2003.
[30] G. Agostini, R. Pellegrini, G. Leofanti, L. Bertinetti, S. Bertarione, E. Groppo, A. Zecchina, C. Lamberti, J. Phys. Chem. C 113 (2009) 10485.
[31] G. Prelazzi, M. Cerboni, G. Leofanti, J. Catal. 181 (1999) 73.
[32] H.G. Fritsche, R.E. Benfield, Z. Phys. D-Atoms Mol. Clusters 26 (1993) S15.
[33] J.M. Montejano-Carrizales, F. Aguilera-Granja, J.L. Moran-Lopez, Nanostruct. Mater. 8 (1997) 269.
[34] W.P. Dow, Y.P. Wang, T.J. Huang, Appl. Catal. A – Gen. 190 (2000) 25.
[35] G.G. Cortez, J.L.G. Fierro, M.A. Banares, Catal. Today 78 (2003) 219.
[36] K. Asano, C. Ohnishi, S. Iwamoto, Y. Shioya, M. Inoue, Appl. Catal. B – Environ. 78 (2008) 242.
[37] S. Bertarione, D. Scarano, A. Zecchina, V. Johanek, J. Hoffmann, S. Schauermann, M.M. Frank, J. Libuda, G. Rupprechter, H.J. Freund, J. Phys. Chem. B 108 (2004) 3603.
[38] G. Spoto, E.N. Gribov, G. Ricchiardi, A. Damin, D. Scarano, S. Bordiga, C. Lamberti, A. Zecchina, Prog. Surf. Sci. 76 (2004) 71.
[39] A.M.J. van der Eerden, T. Visser, A. Nijhuis, Y. Ikeda, M. Lepage, D.C. Koningsberger, B.M. Weckhuysen, J. Am. Chem. Soc. 127 (2005) 3272.
[40] T. Lear, R. Marshall, E.K. Gibson, T. Schutt, T.M. Klapotke, G. Rupprechter, H.J. Freund, J.M. Winfield, D. Lennon, Phys. Chem. Chem. Phys. 7 (2005) 565.
[41] T. Lear, R. Marshall, J.A. Lopez-Sanchez, S.D. Jackson, T.M. Klapotke, M. Baumer, G. Rupprechter, H.J. Freund, D. Lennon, J. Chem. Phys. 123 (2005) (Art. No. 17470).
[42] T. Lear, R. Marshall, J.A. Lopez-Sanchez, S.D. Jackson, T.M. Klapotke, M. Baumer, G. Rupprechter, H.J. Freund, D. Lennon, J. Chem. Phys. 124 (2006) (Art. No. 06990).
[43] S. Bertarione, C. Prestipino, E. Groppo, D. Scarano, G. Spoto, A. Zecchina, R. Pellegrini, G. Leofanti, C. Lamberti, Phys. Chem. Chem. Phys. 8 (2006) 3676.
[44] E. Groppo, S. Bertarione, F. Rotunno, G. Agostini, D. Scarano, R. Pellegrini, G. Leofanti, A. Zecchina, C. Lamberti, J. Phys. Chem. C 111 (2007) 7021.
[45] C. Mondelli, D. Ferri, J.D. Grunwaldt, F. Krumeich, S. Mangold, R. Psaro, A. Baiker, J. Catal. 252 (2007) 77.
[46] D. Tessier, A. Rakai, F. Bozonverduraz, J. Chem. Soc. – Faraday Trans. 88 (1992) 741.
[47] X.P. Xu, D.W. Goodman, J. Phys. Chem. 97 (1993) 7711.
[48] X.P. Xu, P.J. Chen, D.W. Goodman, J. Phys. Chem. 98 (1994) 9242.
[49] H.J. Freund, Angew. Chem. – Int. Edit. Engl. 36 (1997) 452.
[50] K. Wolter, O. Seiferth, J. Libuda, H. Kuhlenbeck, M. Baumer, H.J. Freund, Chem. Phys. Lett. 277 (1997) 513.
[51] K. Wolter, O. Seiferth, J. Libuda, H. Kuhlenbeck, M. Baumer, H.J. Freund, Surf. Sci. 404 (1998) 428.
[52] K. Wolter, O. Seiferth, H. Kuhlenbeck, M. Bäumer, H.J. Freund, Surf. Sci. 399 (1998) 190.
[53] C.R. Henry, Surf. Sci. Rep. 31 (1998) 235.
[54] S. Surnev, M. Sock, M.G. Ramsey, F.P. Netzer, M. Wiklund, M. Borg, J.N. Andersen, Surf. Sci. 470 (2000) 171.
[55] H.J. Freund, M. Baumer, H. Kuhlenbeck, Adv. Catal. 45 (2000) 333.
[56] N. Sheppard, C. De La Cruz, Catal. Today 70 (2001) 3.
[57] E. Ozensoy, D.W. Goodman, Phys. Chem. Chem. Phys. 6 (2004) 3765.
[58] V.E. Henrich, Rep. Prog. Phys. 48 (1985) 1481.
[59] V.E. Henrich, P.A. Cox, in: The Surface Science of Metal Oxides, Cambridge University Press, Cambridge, 1994.
[60] M.A. Barteau, Chem. Rev. 96 (1996) 1413.
[61] M.A. Barteau, J.M. Vohs, in: G. Ertl, H. Knözinger, J. Weitkamp (Eds.), Handbook of Heterogeneous Catalysis, vol. 2, Wiley-VCH, Weinheim, 1997.
[62] C. Xu, D.W. Goodman, in: G. Ertl, H. Knözinger, J. Weitkamp (Eds.), Handbook of Heterogeneous Catalysis, vol. 2, Wiley-VCH, Weinheim, 1997.
[63] L.F. Liotta, G. Deganello, P. Delichere, C. Leclercq, G.A. Martin, J. Catal. 164 (1996) 334.
[64] A.J. Lupinetti, S.H. Strauss, G. Frenking, Prog. Inorg. Chem. 49 (2001) 1.
[65] B.S. Shete, V.S. Kamble, N.M. Gupta, V.B. Kartha, J. Phys. Chem. B 102 (1998) 5581.
[66] E. Garrone, N. Russo, P. Marturano, B. Onida, F. Di Renzo, M. Lasperas, Chem. Commun. (1998) 1717.
[67] H. Praliaud, M. Primet, G.A. Martin, Appl. Surf. Sci. 17 (1983) 107.
[68] P.A.J.M. Angevaare, H.A.C.M. Hendrickx, V. Ponec, J. Catal. 110 (1988) 11.
[69] P.A.J.M. Angevaare, H.A.C.M. Hendrickx, V. Ponec, J. Catal. 110 (1988) 18.
[70] H.W. Wassmuth, J. Ahner, M. Hofer, H. Stolz, Prog. Surf. Sci. 42 (1993) 257.
[71] U. Feuerriegel, W. Klose, S. Sloboshanin, H. Goebel, J.A. Schaefer, Langmuir 10 (1994) 3567.
[72] P.A. Gravil, H. Toulhoat, Surf. Sci. 430 (1999) 176.
[73] L.J. Hu, G.F. Xia, L.L. Qu, M.F. Li, C. Li, Q. Xin, D.D. Li, J. Catal. 202 (2001) 220.
[74] N. Munakata, M. Reinhard, Appl. Catal. B – Environ. 75 (2007) 1.
[75] A. Mori, T. Mizusaki, M. Kawase, T. Maegawa, Y. Monguchi, S. Takao, Y. Takagi, H. Sajiki, Adv. Synth. Catal. 350 (2008) 406.
[76] C.H. Bartholomew, Appl. Catal. A 212 (2001) 17.
[77] A. Zecchina, D. Scarano, S. Bordiga, G. Spoto, C. Lamberti, Adv. Catal. 46 (2001) 265.